Journal of Structural Geology xxx (xxxx) xxx–xxx

Contents lists available at ScienceDirect

Journal of Structural Geology

journal homepage: www.elsevier.com/locate/jsg

Quantitative measures of deformed rocks: The links to dynamics

Alison Ord[a,b,*], Bruce Hobbs[a,c]

[a] Centre for Exploration Targeting, School of Earth Sciences, University of Western Australia, WA, 6009, Australia
[b] School of Resources and Environmental Engineering, Hefei University of Technology, Hefei, 230009, China
[c] CSIRO, Perth, WA, 6102, Australia

ARTICLE INFO

Keywords:
Deformed rocks
Nonlinear analysis
Dynamical systems
Recurrence plots
Recurrence quantification analysis (RQA)

ABSTRACT

One aim of structural geology is to understand the processes that operate during deformation and metamorphism so that the conditions (P, T, strain-rates, stresses, rates of other processes such as grain-size reduction) that control these processes can be identified and quantified. In this paper we explore ways of quantifying the geometry of deformed metamorphic rocks in ways that are directly related to the processes that operated. We propose that structures we observe in nature are the result of coupling between nonlinear processes and hence deforming metamorphic systems behave as nonlinear dynamical systems. As such the descriptions of such systems should utilise the toolbox of methods that have been developed for dynamic systems over the past 50 years or so. These methods include the construction of attractors, multifractal analysis, recurrence plots, recurrence quantification analysis and dynamical network analysis. We illustrate the approach first using numerical models of fold systems, with linear and nonlinear constitutive relations and with and without initially imposed noise (imperfections). We then extend the illustrations to consider natural fold systems. Our conclusions are that the irregularity we see in natural fold systems is the result of nonlinear constitutive laws, not that of initial imperfections and that the number of processes operating to produce the observed fold shapes is relatively small.

1. Introduction

There are two end-member approaches to analysing, quantifying and describing deformation patterns. One is to embrace a linear approach where standard statistical approaches are adopted and one talks about the mean, standard deviation, autocorrelation function, Fourier power spectrum decomposition and other classical measures (Borradaile, 2003). These approaches are parametric, in that an underlying statistical distribution is assumed, and are linear, in that it is assumed that the law of superposition holds, so that any distribution can be usefully represented by the sum of Fourier components (Borradaile, 2003) and kriging or co-kriging are useful ways of interpolating and extrapolating data. These methods force the data to fit an assumed statistical distribution and in doing so commonly discard data ("outliers") that do not belong to that distribution. Low band pass filters are examples of smoothing procedures. These methods of analysis have no intrinsic link to the processes that produced the data.

The second approach is to interrogate the data to see if it has been produced by a nonlinear dynamical system and to employ nonlinear series analysis (Sprott, 2003) in attempting to understand and characterise the underlying dynamics. These methods are non-parametric in that no underlying statistical distributions are assumed and the data "speak for themselves". The methods are equally applicable to linear and nonlinear systems. The tools used include attractor construction in state space (Takens, 1981), recurrence plots and their quantification (Webber and Zbilut, 2005; Marwan et al., 2007b) and recurrence networks (Donner et al., 2010). The emphasis is on deriving the underlying dynamics and processes that produced the data and not on characterising the system with statistical measures. A distinction is made (Stemler and Judd, 2009) between *dynamical noise* which derives from deterministic processes that produced the data and *observational noise* that derives from uncorrelated external sources that are not related to the dynamics. Dynamical noise needs to be preserved whereas observational noise needs to be discarded. This means that all deterministic noise needs to be retained even if parts of this noise seem to constitute "outliers". Such outliers need to be understood, rather than discarded or treated as observational aberrations.

This note concentrates on the nonlinear analysis of folded structures first, to demonstrate how one might measure and, as a result, quantify the departure from linearity of folded structures and second, to provide a field work base-line for future work exploring the consequences for considering nonlinear rather than linear behaviours.

The Biot (1965) theory of buckling has resulted in much research into linear, low amplitude theories for folding. Some (Hudleston and

* Corresponding author. Centre for Exploration Targeting, School of Earth Sciences, University of Western Australia, WA, 6009, Australia.
E-mail address: alison.ord@uwa.edu.au (A. Ord).

https://doi.org/10.1016/j.jsg.2018.05.027
Received 20 December 2017; Received in revised form 10 May 2018; Accepted 28 May 2018

Treagus, 2010) claim that the small amplitude, linear theory of Biot is sufficient to explain all that we see in natural folds and any irregularity we see arises from initial geometrical imperfections in the layer(s). The work of Hunt, Muhlhaus, Hobbs and co-authors over the past 20 years or so (Hunt, 2006; Hunt et al., 1997; Muhlhaus, 1993; Muhlhaus et al., 1998; Hobbs et al., 2009; Hobbs and Ord, 2012) has analysed the constraints of the Biot theory, and discussed folding and other geological structures through nonlinear constitutive relations where irregularities arise naturally through the constitutive relations. This paper uses methods of nonlinear analysis to explore whether the linear or nonlinear approaches are relevant to what we see in nature.

We take as a starting point that the single layer fold profiles we see in natural examples are solutions to the Swift-Hohenberg equation:

$$\frac{\partial w}{\partial t} = \alpha\frac{\partial^4 w}{\partial x^4} + \beta\frac{\partial^2 w}{\partial x^2} + f(w) \tag{1}$$

where $w(x,t)$ is the deflection of a layer during folding measured as the displacement normal to the layer from its initial condition, x is a distance measured along the layer, t is time and α, β are constants.

$f(w)$ is a function that expresses the resistance in the matrix to the deflection of the layer. This expression was solved assuming $f(w)$ to be a linear function of w, by Biot (1965); in this instance the solution is $w = A \sin(x)$ although, because the system is linear, any combination of periodic functions, $w = \sum_i \{A_i \sin(a_i x) + B_i \sin(b_i x)\}$, is also a solution where the A_i, B_i, a_i, b_i are constants including irrational numbers. Thus, in principle, the resultant fold profile could be quite irregular but still readily expressed as a Fourier series. The fundamental contribution made by Biot was to show that one wavelength, the dominant wavelength, grows faster than all others and so the final profile is sinusoidal. If $f(w)$ is nonlinear or is itself a function of time, as is the case if the matrix of the material is a power law viscous material, then (1) has no unique solution (Peletier, 2001; Knobloch, 2008); commonly (Hunt et al., 1997) the solution is a localised fold rather than a sinusoidal fold train. A standard approach (Fletcher, 1974; Johnson and Fletcher, 1994) is to expand the nonlinear constitutive relation as a Taylor series and retain only the linear term. This results in a tractable (linear) problem but the (periodic) solution is only true for deflections small enough that the approximation arising from truncation of the Taylor series remains valid. This generally involves deflections smaller than $\approx 10^{\circ}$. Recent work (Peters et al., 2015; Paesold, 2015) has shown that in general chaotic solutions evolve in mechanical systems with nonlinear constitutive relations and particularly for buckling with large deflections if $f(w)$ is nonlinear.

In most instances nonlinear systems behave as chaotic systems. By this we mean (Small, 2005) that the system is bounded in space and time, that the behaviour is sensitive to initial conditions and that the behaviour is deterministic, being governed by a system of equations that describe the physics and chemical processes that operated. The variables needed to define the operation of the system are called state variables. The behaviour of the system defines an attractor in state space which is the manifold that all states occupy throughout the evolution of the system independently of the initial conditions. The dimension of the space in which this attractor "lives" is the embedding dimension. If one can establish this dimension then one has a constraint on the number of processes that operated. The structures we observe in naturally deformed rocks are a projection into one-, two- or three-dimensions from a higher dimensional space where the attractor "lives".

Natural fold profiles are not strictly periodic and so the periodic solutions to the Swift-Hohenberg equation are proposed to be modified by the influence of initial heterogeneities in the shape of the layer (Hudleston and Treagus, 2010). The null hypothesis we want to test is that natural fold profiles result from periodic or quasi-periodic solutions to the Swift-Hohenberg equation but are modified by initial imperfections in the layer.

2. Approach based on nonlinear dynamics

Nonlinear systems have two important properties that are useful in structural geology. One, due to Poincaré (1890) says that even though a nonlinear system will diverge from its current state, even very strongly, it will recur close to its current state in the future. Here 'close' is measured by some tolerance, ε, commonly referred to as the radius. Thus recurrence is a fundamental property of most nonlinear systems (because they are bounded and deterministic) and some linear systems as well. This paper is concerned with recurrence and ways of quantifying such recurrence in deformed rocks. The other property that arises because the attractor is defined by an indefinitely large number of states is that the system is multifractal (Beck and Schlögl, 1995). We will not explore this avenue in this paper. Examples are given in Ord (1994), Hobbs and Ord (2015), Ord et al. (2016) and Munro et al. (2017). Our emphasis is on recurrence, its visualisation using recurrence plots and its quantification using recurrence quantification analysis (RQA).

2.1. Basic theory: methods of analysis

A powerful theorem known as *Takens' theorem* states that: *the complete dynamics of a system can be derived from a time (or spatial) series for a single state variable from that system*. The reason for this is that in systems where all the state variables are coupled the behaviour of one depends on the behaviours of all the others and so the time or spatial series for one variable has the behaviours of all the other variables encoded within it. The attractor for a system encompasses the dynamics of the system.

Unless the data set pans the entire attractor the results will be less than perfect. Different parts of the attractor, if it is somewhat complicated, will give different results (Small, 2005). See Hobbs and Ord (2015, pp 227–228) for details of the method for constructing an attractor. For a folded surface the procedure for construction of an attractor in two dimensions consists of taking a value for the displacement, w_i, of a layer at a point, x_i, relative to some datum and plotting that displacement against that at another point, $x_{i+\tau}$, a distance τ removed from x_i. τ is called the *delay*. This procedure is repeated for all values of i and $i + \tau$. For an attractor in three dimensions the plot is in $(w_i - w_{i+\tau} - w_{i+2\tau})$ space. Some examples are shown in Fig. 1. Note that one line only of 1D data is derived for analysis, orthogonal to the trends of the folds and for Fig. 1d through 1i, through the middle of the model or specimen. The selection of τ is an art form (Small, 2005). If τ is too small, readings are closely correlated and the resulting attractor is strung out along a diagonal in phase space. The selection of τ should be such that the attractor unfolds off this diagonal (Small, 2005). The attractors in Fig. 1 are the projections of the true attractor into three dimensional space.

Part of the reason why linear parametric procedures fail for nonlinear systems that arise from a number of coupled processes is that in nonlinear systems the data for a particular quantity are a projection of processes from a higher dimensional state space on to that single quantity. Thus for a folding layer the behaviour might be described in a four dimensional state space with coordinates comprising the state variables: strain-rate, stress, temperature, and some expression of a chemical reaction. The final displacements we observe are a projection from the four-dimensional state space on to a one-dimensional spatial series. Quantities that appear close together in the spatial series may in fact be widely separated in state space. Such quantities are called false nearest neighbours and algorithms for calculating these are given by Sprott (2003) and Small (2005). The embedding dimension can be estimated by establishing a space in which the number of false nearest neighbours is a minimum. This is readily undertaken in the VRA software (Kononov, 2006). Details of methods of estimating the embedding dimension are spelt out by Small (2005) together with the pitfalls involved (see also McSharry, 2005).

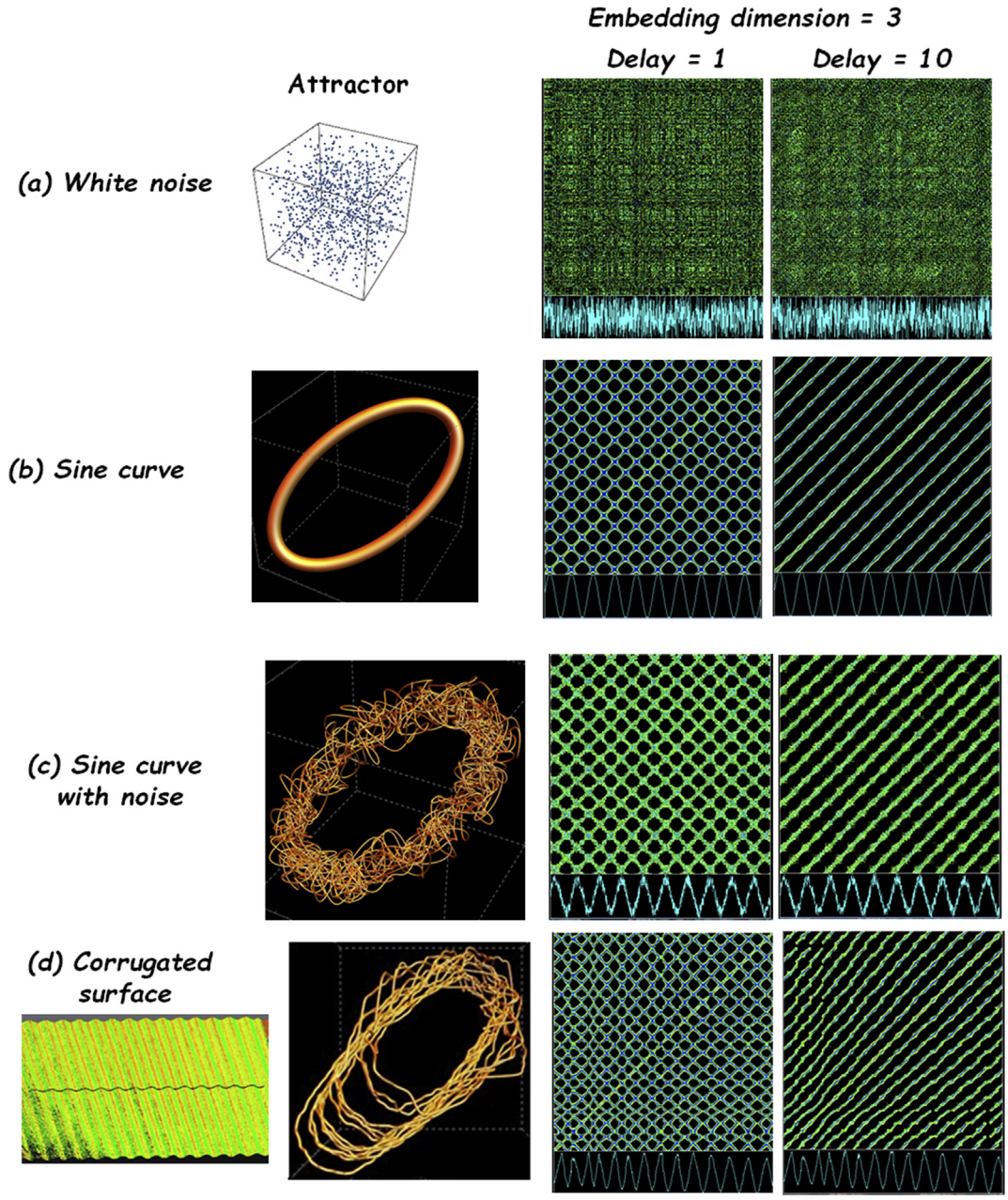

Fig. 1. Specimens (first column), attractors (second column) and recurrence plots with embedding dimension 3 (columns 3: delay = 1 and 4: delay = 10). The signal is beneath each recurrence plot. (a) White noise. (b) Sine curve. (c) Sine curve plus noise (d) Manufactured corrugated sheet. (e) Linear computational system from Hobbs and Ord (2012). (f) Nonlinear computational system from Hobbs and Ord (2012). (g) Crenulated surface, Rum Jungle, Australia. (h) Folded surface, Broken Hill, Australia. (i) Profile of ptygmatic folds supplied by Haakon Fossen.

An important concept in nonlinear analysis is the recurrence plot (Eckmann et al., 1987); this contains all the information that defines the underlying dynamics of a system. A recurrence plot (RP) for a 1 dimensional data set is a symmetrical matrix, R_{ij}, expressed as a two-dimensional visualisation and defined by

$$R_{ij} = \Theta(\varepsilon - \|x_i - x_j\|) \, for \, i, j = 1, \mathrm{N} \tag{2}$$

where ε is an arbitrary threshold distance that measures the radius within which recurrence is identified, Θ is the Heaviside function and $\|*\|$ denotes a norm, commonly taken as the Euclidean norm. (2) says that we measure the distance between a given point, x_i, on the signal and every other point, j = 1 to N on the signal and give that measure the value 1 if the distance is within the radius, ε, or zero if not. This is repeated for all values of i = 1 to N to form the recurrence matrix. The caveat is that the distances are measured in the embedding space. A recurrence plot is then a plot of R_{ij} and may be contoured according to different values of ε. Recurrence plots may also be constructed for higher dimensional data (Vasconcelos et al., 2006; Marwan et al., 2007a) however if the data exists in d-dimensions the recurrence plot is in 2d space. The application of recurrence plots in the geosciences (except for climate studies) is rare; some examples are the application to alteration mineralogy in drill core (Oberst et al., 2017, 2018) and to GNSS data sets (Hobbs and Ord, 2018). The input data are not constrained to any type of statistical distribution and the data are not required to be stationary. There is no need to know the mathematical rules (if any) governing the system under study. The work of Webber (2012) and Kononov (2006) has resulted in software (RQA and VRA respectively; see Belaire-Franch and Contreras, 2002, for a review)

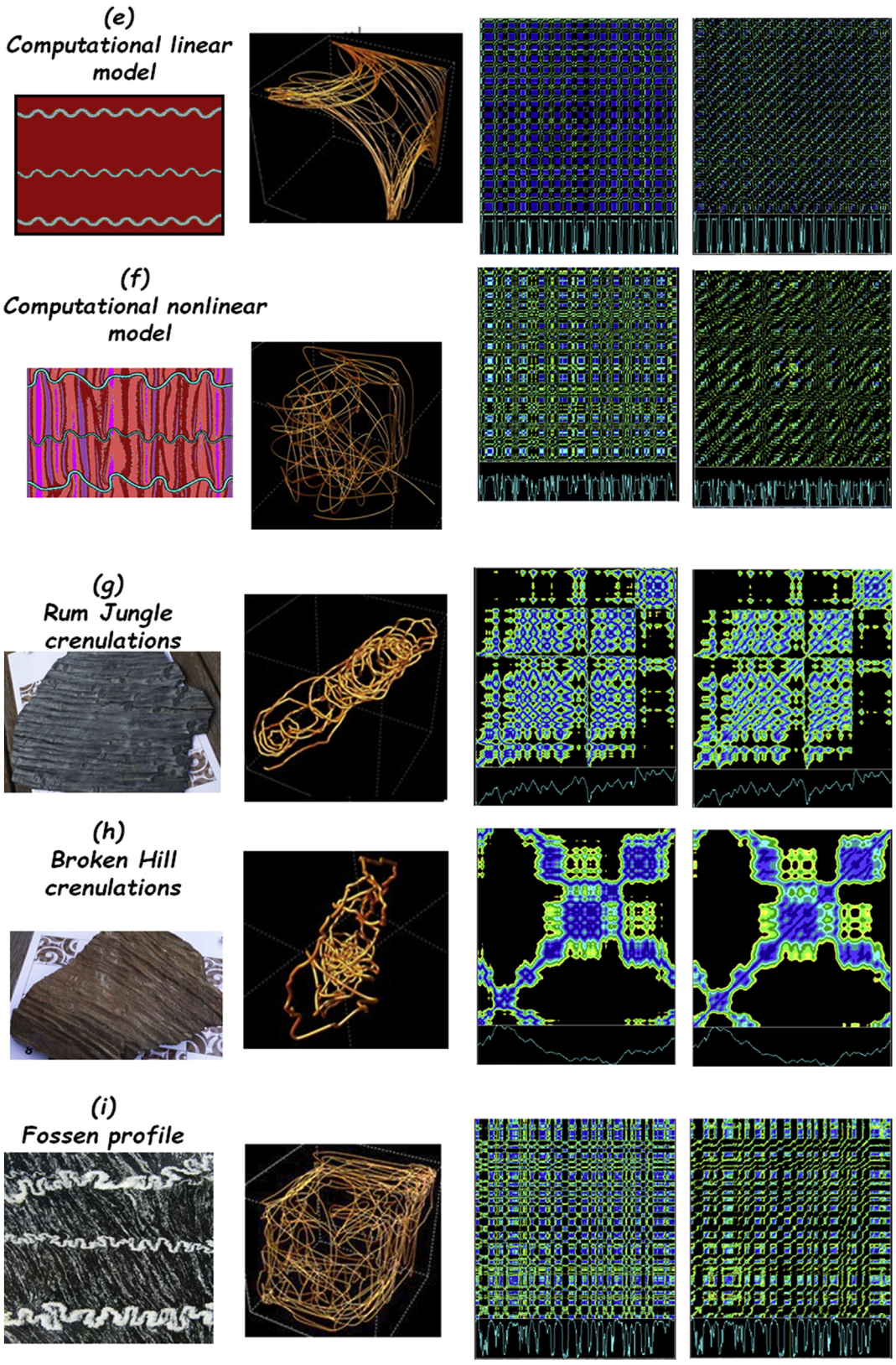

Fig. 1. (*continued*)

which is easily accessible directly through DOS and a Windows operating system. The quantification of recurrence plots has been developed by Webber and Zbilut (2005) and a summary of the various quantification measures with their significance is given in Table 1.

2.2. Prediction and noise

Nonlinear systems exhibit apparently irregular or "noisy" behaviour so that the output from the system (observable data) appears unpredictable and cannot be characterised using Fourier methods. This

Table 1
Definition of recurrence quantification analysis (RQA) measures. (Based on Marwan et al., 2007b).

Measure	Definition
Recurrence rate	The density (percentage) of recurrence points within a given radius in a recurrence plot (RP): $RR = \frac{1}{N^2}\sum_{i,j=1}^{N} R_{ij}$ corresponds with the correlation sum, $C_{2,}$ (where the line of identity [mean diagonal: line of identity, LOI] is excluded). *RR* corresponds with the probability that a specific state will recur. R_{ij} is the recurrence matrix. Single, isolated points represent states are rare &/or exist for a short time &/or fluctuate strongly.
Determinism	The percentage of recurrence points which form diagonal line structures: $DET = \frac{\sum_{l=l_{min}}^{N} lP(l)}{\sum_{l=1}^{N} lP(l)}$ is the histogram of the lengths *l* of the diagonal lines. *DET* is related to the predictability of the dynamical system. The RP for white noise has almost only single dots and very few diagonal lines so that *DET* is low whereas a repeating or deterministic process has an RP with very few single dots but many long diagonal lines. Sine waves will give very long diagonal lines; chaotic signals will give many very short diagonal lines; stochastic signals such as random numbers will give no diagonal lines at all (unless the radius is set too high). A diagonal line represents a segment of the trajectory within phase space which runs almost parallel to another segment
Laminarity	The percentage of recurrence points which form vertical lines: $LAM = \frac{\sum_{v=v_{min}}^{N} vP(v)}{\sum_{v=1}^{N} vP(v)}$ is the histogram of the lengths *v* of the vertical lines. *LAM* reflects the intermittency of the system as laminar states (tangential motion). The state does not change or changes slowly.
Averaged diagonal line length L	The average length of the diagonal lines: $L = \frac{\sum_{l=l_{min}}^{N} lP(l)}{\sum_{l=l_{min}}^{N} P(l)}$ *L* is related to the predictability time of the dynamical system; time that two segments of the trajectory are close to each other; mean prediction time.
Trapping time Trapping size	The average length of the vertical lines: $TT = \frac{\sum_{v=v_{min}}^{N} vP(v)}{\sum_{v=v_{min}}^{N} P(v)}$ *TT* is related to the laminarity time of the dynamical system, or the length of time (or space) the system remains in a specific state, how long the state will be trapped. Vertical lines – define chaos-chaos transitions, chaos-order transitions; investigate intermittency. Trapping size – related to size of area in which system does not change.
Longest diagonal line *LMAX*	The length of the longest diagonal line, equivalent to DMAX in Webber and Zbilut (2005). $Lmax = \max(\{li;\ i = 1,\ldots,Nl\})$ Related to the exponential divergence of the phase space trajectory (the shorter the faster).
Longest vertical line	The length of the longest vertical line, equivalent to *VMAX* in Webber and Zbilut (2005). $Vmax = \max(\{vi;\ i = 1,\ldots,Nv\})$
Divergence	The inverse of *Lmax* $DIV = \frac{1}{Lmax}$ is related to the Kolmogorov-Sinai (*KS)* entropy of the system, that is, to (the sum of) the (largest) positive Lyapunov exponents. Positive Lyapunov exponents gauge the rate at which trajectories diverge, and are the hallmark for dynamic chaos. Thus the shorter the *Lmax*, the more chaotic (less stable) the signal. The higher *DIV*, the faster divergence.
Entropy	The Shannon entropy of the probability distribution of the diagonal line lengths *p(l)*: $ENTR = -\sum_{l=l_{min}}^{N} p(l)\ln p(l)$ *ENTR* reflects the complexity of the deterministic structures in the system. Entropy is expected to be zero for simple periodic systems in which all diagonal lines are of equal length. *ENTR* reflects the complexity of the RP with respect to diagonal lines. Uncorrelated noise has low *ENTR*. $p(l) = P(l)/N_l$ is the probability of finding a diagonal line of exactly length *l* in the recurrence plot.
Trend	The paling or thinning out of the RP towards its edges. Let the recurrence rate of a diagonal line parallel to the LOI and of distance *k* be: $RR_k = \frac{1}{N-k}\sum_{j-1=k}^{N-k} R(i,j)$ then $TREND = \frac{\sum_{i=1}^{\widetilde{N}}(i-\widetilde{N}/2)(RR_i - RR_l)}{\sum_{i=1}^{\widetilde{N}}(i-\widetilde{N}/2)^2}$ *TREND* provides information on the stationarity of the system being near zero for homogeneously distributed recurrent points, and non-zero for a heterogeneous distribution. Fading to the upper left and lower right corners signifies a trend or a drift. *TREND* tends to zero for an homogeneous distribution and to infinity with an heterogeneous distribution.

N – total number of points on the phase space trajectory.
N_l – total number of diagonal lines in the recurrence plot $N_l = \sum_{l>l_{min}} P(l)$.
N_v – total number of vertical lines in the recurrence plot.
P(*l*), P(*v*) – histogram or frequency distribution of the line lengths of diagonal/vertical lines.
$\widetilde{N}$ - maximal number of diagonals parallel to the LOI considered for the calculation of TREND $\widetilde{N} < N$.
$\langle\cdot\rangle$ represents the average value.

output commonly results from two processes of which one may dominate over the other. The signal results from deterministic processes such as mechanical deformation or chemical reactions that define the dynamics of the system and are expressed by a system of coupled differential equations that we write as $\boldsymbol{g}(\boldsymbol{x}, t)$. In many systems other processes operate that are still deterministic but are much noisier; we call the product $\boldsymbol{u}(\boldsymbol{x}, t)$; this is dynamical noise. Dynamical noise results when two competing deterministic processes operate on different time or spatial scales to spread or shift the probability distribution of some quantity of interest such as fold amplitude or grain size. The result (Stemler and Judd, 2009) is a system that operates in space (with coordinates, $\boldsymbol{x}$) and time as

$$\boldsymbol{s}(\boldsymbol{x}, t) = \boldsymbol{g}(\boldsymbol{x}, t) + \boldsymbol{u}(\boldsymbol{x}, t)$$

We make observations, $\boldsymbol{o}(\boldsymbol{x}, t)$, on this system:

$$\boldsymbol{o}(\boldsymbol{x}, t) = \boldsymbol{h}(\boldsymbol{x}, t) + \boldsymbol{n}(\boldsymbol{x}, t)$$

where $\boldsymbol{h}(\boldsymbol{x}, t)$ is the spatial and temporal signal produced by the system and $\boldsymbol{n}(\boldsymbol{x}, t)$ is uncorrelated noise imposed by external sources and has no influence on the dynamics; this is observational noise. In attempting to understand the operation of such systems we need to determine the functions $\boldsymbol{g}(\boldsymbol{x}, t)$, retain the dynamical noise and remove the observational noise.

The process of nonlinear noise reduction is essentially the inverse of the prediction (or forecasting) problem. For nonlinear noise reduction one determines the dynamics of the system given the whole signal up to its current state and then searches for parts of the signal in the past that are not part of the dynamics. These parts are removed as noise. This means we take the whole signal and work backwards. For prediction we take one part of the signal, determine the dynamics and then see if we can find a part of the dynamics that fits the way in which the signal is evolving into the future and use that to make a forward prediction or forecast. Such a procedure is a good way of testing if a model that has been developed for a system is reasonable. An example of prediction is given in Hobbs and Ord (2018).

3. Folding as an example

The data for the surfaces explored in this note are obtained through a general photogrammetric procedure similar to the method described by Thiele et al. (2015), resulting in a dense point cloud of (x, y, z) coordinates for the rock surface. In this paper a line of best fit is then established for the point cloud and that profile is analysed using recurrence plots.

3.1. Data analysis

Two types of data are analysed, one type comprises folds produced analytically, computationally or engineered, and the other, folds observed as natural examples. In each case, a line only of 1D data is derived for analysis, being a section of the folds represented by grey-scale or by amplitude. There is vast room for future analysis of folded systems in 2D and 3D.

Fig. 1 displays the attractor (column 2) and 2 sets of recurrence plots (columns 3 and 4) for the data in column 1: (a) white noise data, (b) a sine curve, (c) a sine curve with noise (d) an engineered corrugated surface (e) a computationally linear fold, (f) a computationally nonlinear fold, (g) and (h) two naturally folded surfaces, one from Rum Jungle, Australia, and the other from Broken Hill, Australia, and (i) a profile of three folded surfaces with a differentiated axial plane structure generously supplied by Haakon Fossen. For the sake of comparison the embedding dimension for each recurrence plot is 3 with a delay, τ, of 1 (column 3) and 10 (column 4). In Table 2 we show the RQA results for each data set.

The attractor for the random data (Fig. 1a) continues to fill space, and the recurrence plots continue to show random distributions of points (with some occasional minor structure by chance), irrespective of the size of the embedding dimension or of the delay. The recurrence rate and the determinism or predictability are low, as is the entropy, which is to be expected for uncorrelated noise. Trend tends to zero, as expected for a homogeneous distribution of recurrence points. Laminarity is low, again as is to be expected, and distinguishes the random data from all other data analysed. The low values of all RQA measures distinguishes this data set from all other examples.

Table 2
Results of RQA for an assumed embedding dimension of 3 and a delay of 10.

Data set	%Rec	%Det	Lmax	Entropy	Trend	%Lam	Vmax	Ttime
white noise	9.2	17.1	6	0.5	−0.6	19.7	4	2.1
Sine	17	100	979	3.5	−3.8	99.9	21	15.2
Sine + noise	18.3	82.8	142	3.0	−3.1	87.3	30	6
Corrugated	22	99.3	1674	6.2	0.4	99.9	62	25.4
Linear	15.5	76.5	49	2.3	3.1	87.7	14	4
Nonlinear	13.4	71.8	33	2.2	0.2	83.4	26	3.9
Rum Jungle	47.4	99.9	2187	7.6	−43.1	100	754	101.1
Broken Hill	40.2	99.9	1241	7.6	−56.4	100	592	121.8
Fossen	28.4	99.2	1458	5.1	2.4	99.6	234	24.9

The attractor for the sine curve (Fig. 1b) is a slim or broad ellipse, depending on the magnitude of the delay, but is only ever two-dimensional. Noise added to the sine curve (Fig. 1c) adds a roughness to the ellipse, and the overall topology is changed because knots are added to the ellipse indicating that false neighbours have been added. The differences between the attractors for sine and sine plus noise illustrate the influence of noise in increasing the embedding dimension. Determinism is high, again as is to be expected, with long diagonals in the recurrence plots. Trend tends to be small, as expected for a homogeneous distribution of recurrence points.

The corrugated sheet (Fig. 1d) looks, by eye, to be of sinusoidal form. The attractor appears to be formed of multiple ellipses rather than the single ellipse for the sine curve, possibly a result of imperfections in the engineering of the sheet. The associated embedding dimension is 2–5, possibly also as a result of such imperfections. Both recurrence plots are very similar to those for the sine curve and the sine curve with noise but with notable distortions in the pattern.

The linear “sinusoidal” curve (Fig. 1e) of Hobbs and Ord (2012; data from horizontal line, centre of figure) has an attractor with an embedding dimension of 2–4. The recurrence plots at low delay ($\tau = 1$), show a pattern that is strongly periodic as for the sine curve with noise; at larger delays ($\tau = 10$), diagonal lines are well developed, as for the sine curve with noise. Thus although the computational solution to (1) for a linear $f(w)$ is supposed to be sinusoidal and appears as such to the eye, the recurrence plots show discernible contributions from noise perhaps arising from the initial distribution of imperfections added in the computational procedure.

However, the nonlinear curve (Fig. 1f) of Hobbs and Ord (2012) has an attractor with an embedding dimension of 3–8, which can be seen in three dimensions to have many cross-cutting structures not seen in the attractors for the sine curve or the sine curve with noise. Such structures or transitions are typical of chaotic systems that spend relatively large amounts of time on one part of an attractor and then jump to another part of the attractor. The trapping time is a measure of how long it spends at one point on the attractor. Such chaotic transitions are strong in this recurrence plot and, with the higher delay, short diagonal lines express the reduced determinism of this model.

The Rum Jungle specimen (Ord et al., 1991) has an attractor displaying intertwined ellipses (Fig. 1g). The attractor has a remarkably high embedding dimension of about 6. The intertwined ellipses result in part from non-stationary behaviour as observed in the two recurrence plots, which look remarkably similar despite the differences in delay. The main transitions are the same, and determinism does not increase with the delay.

The Broken Hill rock (Fig. 1h), despite its apparent complexity, particularly of the attractor, has an embedding dimension only of 2–3. The recurrence plots demonstrate the non-stationary behaviour of the data, reflecting the obvious large scale fold on which are imposed parasitic folds. The figure (delay 1 embedding dimension 3) is dominated by structural blocks surrounding the line of identity (LOI; Table 1).

Increasing the delay only, to 10, results in some of the smaller contour levels becoming diagonal lines. RQA measures for both Rum Jungle and Broken Hill specimens are similar but significantly different to other non-natural examples.

The Fossen specimen (Fig. 1i) has been analysed in a similar manner to the two computational curves described above. The embedding

dimension is 4–10, the form of the attractor and the patterns of the recurrence plots are remarkably similar to those of the computational nonlinear curve (Fig. 1f) even though the RQA measures are substantially different.

4. Discussion

The aim of this paper is to introduce the concept of nonlinear dynamical analysis into structural geology with particular emphasis on recurrence plots and their quantification. Methods based on nonlinear dynamics provide a powerful procedure for quantifying naturally deformed rocks and in deriving the processes responsible for their formation. The application described in this paper is to fold systems and is meant to explore the null hypothesis that natural fold systems form in ways described by the linear Biot theory of buckling and that any irregularities in the resultant folds result from initial imperfections in the layers. If observations do not match this hypothesis it needs to be abandoned and other explanations, compatible with the observations are required.

What do we expect from the null hypothesis? The recurrence plot for a system derived from periodic solutions to (1) with imposed initial noise consists of continuous diagonal lines (for strict periodicity) or quasi-periodic[1] patterns for quasi-periodic profiles. The addition of noise means these patterns are smeared somewhat and large amplitude initial imperfections of periodic or quasi-periodic nature will introduce decorations on diagonal lines or new short segments of diagonal lines but no vertical lines in the recurrence plot. Since the addition of initial imperfections means the fold profiles remain periodic or quasi-periodic (perhaps disrupted by noise) the determinism of the system should always be high and the Lyapunov exponent small or even negative. The entropy should always be low and vmax and traptime small. The embedding dimension of the attractor should be small (say 2 to 4).

What does the recurrence analysis show? The Rum Jungle and Broken Hill specimens differ remarkably in the nature of their recurrence plots from the sine, sine + noise and corrugated examples recurrence plots. Part of this results from non-stationary behaviour for the natural examples but the natural examples have high values of trap time and vmax which indicates a tendency for chaotic transitions over the synthetic examples. %recurrence and entropy are also significantly higher for the natural examples. The embedding dimension for Rum Jungle is high (~6) although that for the Broken Hill specimen is low (~2–3). These features are not what is expected of a sinusoidal (or quasi-periodic) system with local initial imperfections in the folded layer but are consistent with chaotic behaviour in a nonlinear system.

The Fossen specimen has been analysed in a different way to the other two natural examples but again has higher %recurrence, entropy vmax and trap time than is to be expected from sinusoidal system with local imperfections. It is remarkable how similar the recurrence plot for the Fossen specimen is to the nonlinear computational model although such similarity is not reflected in the RQA. Overall the recurrence characteristics of natural specimens have little in common with the same characteristics for synthetic and computational models indicating that more realistic processes need to be built into these models before some degree of realism is achieved.

4.1. Future developments

The application of photogrammetry to capture the three dimensional fabric of deformed rocks together with nonlinear analysis provides methods based on nonlinear dynamics to quantifying and classify naturally deformed rocks according to the processes responsible for their formation. Recurrence Quantification Analysis provides tools for predicting patterns of folding and fracturing ahead of drilling and mining, for quantifying uncertainty, and for creating geological maps of the distribution of RQA measures. For geotechnical applications, Ord et al. (1991) note that the spatial distribution of the rock surface is obtained by cross-correlating the (x, y, z) coordinates across the surface and by describing a spatial attractor. The information contained within this attractor may be compared with that generated by numerical models of jointing and deformation with the aim of more fully comprehending fundamental rock behaviour. Nonlinear analysis and prediction is fundamental for rock engineering purposes (Hobbs, 1993). The spatial attractors possess all the geometrical information necessary to discuss the spatial correlations between structures and thus form the basis for defining the probability whether a particular structure will exist at a specified point or not and whether these structural geometries are deterministic and derive from well-defined dynamical relations so can be used for nonlinear prediction. This injects a level of understanding that has always been lacking and sets the scene for future studies of the origins and forms of geometrical complexity in these structures. Insight into the dynamic processes inferred from patterns is a benefit of this RQA analytical approach.

5. Conclusions

We have presented the basic aspects of the nonlinear analysis of geological fabrics. In particular recurrence plots and their quantification provide the basis for characterising and classifying fabrics based on the processes that formed the fabrics. As an example we show that the irregularity we see in natural fold systems is consistent with an origin derived from nonlinear constitutive laws and is not consistent with an origin derived from initial imperfections. Initial random or periodic/quasi-periodic imperfections result in recurrence plots with low values of entropy, vmax and trap time. Natural folds exhibit high values of these measures indicating that the observed irregularity derives from underlying chaotic dynamics. They demonstrate significant chaotic transitions which do not exist in periodic or quasi-periodic structures.

Methods based on nonlinear dynamics provide a powerful procedure for quantifying naturally deformed rocks, in deriving the processes responsible for their formation, in undertaking interpolation and extrapolation of data and in quantifying uncertainty. Their applications in metamorphic geology and structural geology in particular will provide significant advances in knowledge.

Johnson and Fletcher (1994; Footnote 3, page 353) note: 'We might add that, if you long for a humbling experience … merely compare the forms of your theoretical fold forms, simulated in viscous (or elastic) materials, with the forms of some actual folds!' The methods outlined in this paper provide ways of performing such comparisons.

Acknowledgements

We thank Klaus Gessner and Greg Dering for work in digitising the rock surfaces and Sebastian Oberst and Robert Niven for introducing us to recurrence plots.

References

Beck, C., Schlögl, F., 1995. Thermodynamics of Chaotic Systems. Cambridge University Press, New York.

Belaire-Franch, J., Contreras, D., 2002. Recurrence plots in nonlinear time series analysis: free software. J. Stat. Software 7, 1–18.

Biot, M.A., 1965. Mechanics of Incremental Deformations. John Wiley, New York.

Borradaile, G.J., 2003. Statistics of Earth Science Data. Springer-Verlag Berlin.

Donner, R.V., Zou, Y., Donges, J.F., Marwan, N., Kurths, J., 2010. Recurrence networks- a novel paradigm for nonlinear time series analysis. N. J. Phys. 12, 033025 1- 40.

Eckmann, J.-P., Kamphorst, S.O., Ruelle, D., 1987. Recurrence plots of dynamical systems. Europhys. Lett. 4, 973–977.

Fletcher, R.C., 1974. Wavelength selection in folding of a single layer with power law rheology. Am. J. Sci. 274 1029 - !043.

Hobbs, B.E., 1993. The significance of structural geology in rock mechanics (Chapter 2) In: In: Hoek, E., Hudson, J., Brown, E.T. (Eds.), Comprehensive Rock Engineering,

[1] A quasi-periodic signal is one that almost repeats itself but never does. It results from equations of the type $y = a\sin(\alpha x) + b\sin(\beta x)$ where the ratio, $\alpha{:}\beta$, is irrational.

vol. 1. Pergamon Press, pp. 25–62.
Hobbs, B.E., Ord, A., 2012. Localized and chaotic folding: the role of axial plane structures. Phil. Trans. R. Soc. A 370, 1966–2009.
Hobbs, B.E., Ord, A., 2015. Structural Geology: the Mechanics of Deforming Metamorphic Rocks. Elsevier, Netherlands.
Hobbs, B.E., Ord, A., 2018. Nonlinear dynamical analysis of GNSS data: quantification, precursors and synchronization. Prog. Earth Planet. Sci (in review) 2018.
Hobbs, B.E., Regenauer-Lieb, K., Ord, A., 2009. Folding with thermal-mechanical feedback; A reply. J. Struct. Geol. 31, 540–543.
Hudleston, P.J., Treagus, S.H., 2010. Information from folds; a review. J. Struct. Geol. 32, 2042–2071.
Hunt, G.W., 2006. Buckling in space and time. Nonlinear Dynam. 43, 29–46.
Hunt, G.W., Muhlhaus, H.-B., Whiting, I.M., 1997. Folding processes and solitary waves in structural geology. Phil. Trans. Roy. Soc. Series A 355, 2197–2213.
Johnson, A.M., Fletcher, R.C., 1994. Folding of Viscous Layers. Columbia University Press, New York.
Knobloch, E., 2008. Spatially localised structures in dissipative systems: open problems. Nonlinearity 21, T45–T60.
Kononov, E., 2006. VRA Visual Recurrence Analysis. http://web.archive.org/web/20070131023353/http://www.myjavaserver.com/~nonlinear/vra/download.html, 4.9.
Marwan, N., Kurths, J., Saparin, P., 2007a. Generalised recurrence plot analysis for spatial data. Phys. Lett. A 360, 545–551.
Marwan, N., Roman, M.C., Thiel, M., Kurths, J., 2007b. Recurrence plots for the analysis of complex systems. Phys. Rep. 438, 237–329.
McSharry, P., 2005. The danger of wishing for chaos. Nonlinear Dynam. Psychol. Life Sci. 9, 375–397.
Muhlhaus, H.-B., 1993. Evolution of elastic folds in plane strain. In: Kolymbas, D. (Ed.), Modern Approaches to Plasticity. Elsevier Science Publishers B.V, pp. 737–765.
Muhlhaus, H.-B., Sakaguchi, H., Hobbs, B.E., 1998. Evolution of three-dimensional folds for a non-Newtonian plate in a viscous medium. Proc. Roy. Soc. Lond. 454, 3121–3143.
Munro, M.A., Ord, A., Hobbs, B.E., 2017. Spatial organization of gold and alteration mineralogy in hydrothermal systems: wavelet analysis of drill core from Sunrise Dam Gold Mine, Western Australia. In: Gessner, K., Blenkinsop, T.G., Sorjonen-Ward, P. (Eds.), Characterization of Ore-forming Systems from Geological, Geochemical and Geophysical Studies. Geological Society, London, Special Publications, pp. 453.
Oberst, S., Niven, R., Ord, A., Hobbs, B., Lester, D., 2017. Application of recurrence plots to orebody exploration data. 114-116. In: Wyche, S., Witt, W.K. (Eds.), TARGET 2017, Perth, Australia: Abstracts. Geological Survey of Western Australia Record 2017/6, 166p.
Oberst, S., Niven, R., Lester, D., Ord, A., Hobbs, B., Hoffmann, N., 2018. Detection of unstable periodic orbits in mineralizing geological systems. Chaos. In review.
Ord, A., Cheung, L.C., Hobbs, B.E., Le Blanc, D., 1991. Automatic mapping of rock exposures for geotechnical purposes. In: Baafi, E.Y. (Ed.), 2nd Aust. Conf. on Computer Applications in the Mineral Industry. Univ. of Wollongong, pp. 205–210.
Ord, A., 1994. The fractal geometry of patterned structures in numerical models for rock deformation. In: Krühl, J.H. (Ed.), Fractals and Dynamic Systems in Geoscience. Springer-Verlag, Berlin, pp. 131–155.
Ord, A., Munro, M., Hobbs, B.E., 2016. Hydrothermal mineralising systems as chemical reactors: wavelet analysis, multifractals and correlations. Ore Geol. Rev. 79, 155–179.
Paesold, M.K., 2015. Localization Phenomena in Geological Settings. PhD thesis. The University of Western Australia.
Peletier, M.A., 2001. Sequential buckling: a variational analysis. SIAM J. Math. Anal. 32, 1142–1168.
Peters, M., Veveakis, M., Poulet, T., Karrech, A., Herwegh, M., Regenauer-Lieb, K., 2015. Boudinage as a material instability of elasto-visco-plastic rocks. J. Struct. Geol. 78, 86–102.
Poincaré, H., 1890. Sur le problème des trois corps et les équations de la dynamique. Acta Math. 13, 1–271.
Small, M., 2005. Applied Nonlinear Time Series Analysis: Applications in Physics, Physiology and Finance. World Scientific, Singapore.
Sprott, J.C., 2003. Chaos and Time Series Analysis. Oxford University Press, Oxford 507 pp.
Stemler, T., Judd, K., 2009. A guide to using shadowing filters for forecasting and state estimation. Physica D 238, 1260–1273.
Takens, F., 1981. Detecting strange attractors in turbulence. In: In: Rand, D., Young, L.-S. (Eds.), Dynamical Systems and Turbulence. Lecture Notes in Mathematics, vol. 898. pp. 366–381.
Thiele, S.T., Micklethwaite, S., Bourke, P., Verrall, M., Kovesi, P., 2015. Insights into the mechanics of en-echelon sigmoidal vein formation using ultra-high resolution photogrammetry and computed tomography. J. Struct. Geol. 77, 27–44.
Vasconcelos, D.B., Lopes, S.R., Viana, R.L., Kurths, J., 2006. Spatial recurrence plots. Phys. Rev. E 73, 056207.
Webber Jr., C.L., 2012. README_2012.PDF (Introduction to Recurrence Quantification Analysis, V 14.1). http://homepages.luc.edu/~cwebber.
Webber Jr., C.L., Zbilut, J.P., 2005. Recurrence quantification analysis of nonlinear dynamical systems. In: Riley, M.A., Van Orden, G. (Eds.), Tutorials in Contemporary Nonlinear Methods for the Behavioral Sciences, pp. 26–94. (Chapter 2). http://www.nsf.gov/sbe/bcs/pac/nmbs/nmbs.pdf.